AGU PUBLICATIONS

Space Weather

RESEARCH ARTICLE
10.1002/2016SW001545

Key Points:
- Coronagraphs can be used for SEP warnings
- The instrument needed for SEP warnings is different from the one needed to forecast geomagnetic storms
- The primary component of a prototype coronagraph warning system for SEPs exists today

Correspondence to:
O. C. St. Cyr,
Chris.StCyr@nasa.gov

Citation:
St. Cyr, O. C., A. Posner, and J. T. Burkepile (2017), Solar energetic particle warnings from a coronagraph, *Space Weather*, *15*, 240–257, doi:10.1002/2016SW001545.

Received 5 OCT 2016
Accepted 8 JAN 2017
Accepted article online 10 JAN 2017
Published online 30 JAN 2017

Solar energetic particle warnings from a coronagraph

O. C. St. Cyr[1], A. Posner[2], and J. T. Burkepile[3]

[1]NASA-GSFC, Greenbelt, Maryland, USA, [2]NASA-HQ, Washington, District of Columbia, USA, [3]HAO/NCAR, Boulder, Colorado, USA

Abstract We report here the concept of using near-real time observations from a coronagraph to provide early warning of a fast coronal mass ejection (CME) and the possible onset of a solar energetic particle (SEP) event. The 1 January 2016, fast CME, and its associated SEP event are cited as an example. The CME was detected by the ground-based K-Cor coronagraph at Mauna Loa Solar Observatory and by the SOHO Large Angle and Spectrometric Coronagraph. The near-real-time availability of the high-cadence K-Cor observations in the low corona leads to an obvious question: "Why has no one attempted to use a coronagraph as an early warning device for SEP events?" The answer is that the low image cadence and the long latency of existing spaceborne coronagraphs make them valid for archival studies but typically unsuitable for near-real-time forecasting. The January 2016 event provided favorable CME viewing geometry and demonstrated that the primary component of a prototype ground-based system for SEP warnings is available several hours on most days. We discuss how a conceptual CME-based warning system relates to other techniques, including an estimate of the relative SEP warning times, and how such a system might be realized.

1. Introduction

The first report that the Sun could produce and release energetic particles was made by *Forbush* [1946]. He observed three separate enhancements in ground-based measurements of the cosmic radiation background, and he put forth the idea that the charged particle increases might be from the Sun. A decade after Forbush, concerted efforts to understand the space environment as part of the International Geophysical Year led to expanded observations of solar energetic particles (SEPs) from balloons [e.g., *Anderson et al*., 1959] and spacecraft [e.g., *Arnoldy et al*., 1960]. With the new understanding came the realization that both human [e.g., *Pickering and Talbot*, 1963] and robotic explorers [e.g., *Prew*, 1956] would be susceptible to the effects of radiation. In 1966, the Proton Flare Project [e.g., *Svestka and Simon*, 1969] focused international observatories on a solar-observing campaign for several months to try to understand the phenomena.

English et al. [1973] outlined the spaceflight rules that were in effect for the *Apollo* manned missions to the Moon, and they described the *Solar Particle Alert Network* consisting of multiple-frequency radio telescopes and optical telescopes that were operated under contract to NASA. A more recent summary of the radiation risks in spaceflight and recommendations to address them were compiled by the *National Research Council* [2008], and many researchers have already been thinking about this hazard to human interplanetary space travel [e.g., *McKenna-Lawlor et al*., 2012; *Kim et al*., 2014]. In fact, one of the National Research Council recommendations was that the forecasting and warning of SEP events should be an essential part of a comprehensive radiation mitigation strategy. Additional societal effects of solar X-ray and SEP events are terrestrial polar cap absorption events [e.g., *Bailey*, 1957; *Warwick and Haurwitz*, 1962; *Reid*, 1972], which can severely disrupt HF radio communications and lead to rerouting of over-the-pole commercial airline flights. Harmful levels of SEPs have even been reported at commercial airline altitudes, potentially exposing crews and passengers to health risks [e.g., *Mertens et al*., 2010].

Energetic particle events are usually described as being SEPs, referring to particles accelerated close to the Sun and streaming to the observer, or as energetic storm particle (ESP) events, referring to particles accelerated at a distance from the Sun by shocks/compressions in the solar wind. The ESP events often peak at or near shock passage, and *Cohen et al*. [2001] reported that measurements from the Lagrangian L1 point can provide 30–60 min forecast of these particles that have been accelerated at strong interplanetary shocks. In this manuscript we focus on SEPs and their forecasting techniques, and we exclude ESP events from further discussion.

More than five decades of space-based observations have passed, but the role of particle acceleration in flares and coronal mass ejections (CMEs) contributing to SEP events is still under debate. Before the discovery of CMEs in the early 1970s, SEPs were thought to originate solely, or at least predominantly, from flares in active regions, and this is reflected in the formulation of SEP prediction techniques at that time. In addition, both type III (escaping electrons) and type II (shock-induced radiation at the local plasma frequency) solar radio bursts were incorporated into prediction schemes. After the discovery of CMEs in images from the Orbiting Solar Observatory 7 coronagraph [*Tousey and Koomen*, 1972], and the compilation of a large sample of CMEs was obtained with Skylab ATM S-052 [e.g., *Gosling et al*., 1974], associations of SEPs with CMEs were then recognized. The first report of a link between CMEs and SEPs was made by *Kahler et al*. [1978]. That work was extended by *Kahler et al*. [1984] and by *Cane et al*. [1988], who noted that the intensity profiles of SEP events were tied to heliolongitude and to the extent of interplanetary shocks near the Sun. *Cane et al*. [2002] reported that all >20 MeV SEP events were preceded by type-III *l* radio bursts ("*l*" referring to longer duration) and associated CMEs. Earlier *McCracken* [1962] had explained the preference for prompt SEPs to the western hemisphere as being due to propagation effects rather than production conditions. While most SEP events appear to be associated with large flares and fast CMEs, the reverse is not true [e.g., *Cliver et al*., 2012, Figure 1].

The large angular span of heliolongitude for some SEP events was known from Helios observations in the late 1970s [e.g., *McGuire et al*., 1983]. More recently, multipoint measurements at various radial distances have confirmed the large spread of some events [e.g., *Prise et al*., 2014; *Dresing et al*., 2012; *Richardson et al*., 2014]. Significantly different (inferred) speeds of azimuthal transport for electrons and protons were also known from Helios observations [e.g., *Kallenrode*, 1993], and they were confirmed with three-point STEREO and near-Earth observations at 1 AU distance from the Sun [*Richardson et al*., 2014]. Ulysses observations confirm that SEPs can also extend to high latitudes [e.g., *Dalla et al*., 2003]. But the location(s) of the acceleration and azimuthal transport for SEPs remains an open question. With the discovery of the connection between CMEs and propagating EUV dimmings and waves in the low corona [e.g., *Thompson et al*., 1998], it appeared that an answer to the azimuthal transport of SEPs might be at hand [e.g., *Rouillard et al*., 2011, 2012]. But more recent studies now indicate that it may be the transit of the shock at higher altitudes (>2 R_{Sun}), associated with the white-light CME rather than the EUV wave, that allows SEPs to access interplanetary magnetic field lines far from the flare site [e.g., *Lario et al*., 2014, 2016]. While this process may work for protons, the *Richardson et al*. [2014] report, as well as an earlier report by *Posner et al*. [1997], indicates that it cannot also account for electrons, whose source speed and onset delay do not match the EUV wave. *Dierckxsens et al*. [2015] compared the statistics of SEP proton events at two different energies (>10 MeV and >60 MeV) with flare and CME characteristics. They reported that the correlation of SEPs with flare intensity increases with energy, while the correlation with CME speed does the opposite. They speculated that this behavior may indicate a mixed SEP origin, where both flare- and CME shock-driven acceleration contribute. Despite this lack of closure, we will show that the combination of early CME detection with respect to SEP onset, and fast and effective longitudinal particle transport away from the CME longitude, allow us to test a SEP forecasting scheme based on CME observations.

It is known that fast (i.e., >800 km/s) CMEs are more likely than slower CMEs to be associated with SEP events; however, for a given CME speed, the SEP intensity can vary over 3 orders of magnitude [e.g., *Reames*, 2000; *Kahler*, 2001]. *Gopalswamy et al*. [2008] reported on fast and wide CMEs observed by SOHO Large Angle and Spectrometric Coronagraph (LASCO) [*Brueckner et al*., 1995] between 1996 and 2005. They found that the SEP association rate increased linearly with CME speed from about 30% for 800 km/s CMEs, up to 100% for CMEs traveling ≥1800 km/s, for those events that were magnetically well connected to Earth and had accompanying decameter-hectometer (DH) type II radio bursts. They also noted that no large SEP events are associated with radio-quiet CMEs (those without type II bursts) and that only about half of the fast and wide CMEs with accompanying radio bursts are associated with SEPs. The preference for SEPs to accompany fast CMEs with DH type II over metric type II radio bursts had also been reported by *Cliver et al*. [2004], who argued that shocks that survive beyond ~3 R_{Sun} would be more likely to have broad azimuthal extent. The *Gopalswamy et al*. [2008] result has been confirmed and extended by examining CMEs associated with magnetically well-connected SEP events at Earth, as well as at the twin STEREO spacecraft at widely separated heliolongitudes (Yashiro, personal communication, 2016).

In this manuscript we introduce the concept of using near-real-time observations from a coronagraph to provide a warning of the onset of an SEP event. We structure this manuscript as follows: we first review existing SEP forecasting techniques, and then we discuss the observations of the 1 January 2016 SEP CME and associated activity; we then compare the SEP warning time for this event from the coronagraphs and other techniques. In section 5, we briefly review what is known about CME dynamics in the low corona, which allows us to estimate the SEP warning that is possible from a coronagraph. Finally, we imagine how a robust coronagraph-based warning system might be realized.

2. Existing SEP Forecasting Techniques

Historically, there have been several techniques employed to predict a variety of parameters for SEPs (although each technique may forecast only a subset of those parameters) that may include the time of onset, the time and intensity of peak flux, duration, and some spectral characteristics. One standard in forecasting techniques is that the peak flux intensity is frequently expressed using the NOAA Space Weather Prediction Center (SWPC) "*S*" scale of solar radiation storm impacts, which has decadal thresholds of 10, 100, … 10^5 proton flux units (pfu or particles $cm^{-2}\,s^{-1}\,sr^{-1}$) as measured by GOES 5 min averaged integral flux for ≥10 MeV, ≥50 MeV, and ≥100 MeV protons. SWPC proton event *warnings* are forecasts of an impending SEP onset, and *alerts* are issued when one of the thresholds is exceeded. The interested reader can refer to the detailed description of warnings/alerts and the impacts online at http://www.swpc.noaa.gov/products/goes-proton-flux. (A note of caution: the terrestrial weather community uses the terminology *watches* and *warnings* in forecasts of severe weather; we speculate that this will be a source of confusion in the future as the space weather and tropospheric forecasting communities continue to explore their interconnectivity [e.g., *Jackman et al*., 2000]).

An early SEP forecasting technique was claimed by *Castelli et al*. [1967], who reported that a preferred "*U* shape" in the spectrum in solar microwave radio bursts was a reliable predictor of energetic proton activity. Additional reports by *Castelli and Barron* [1977] and by *Bakshi and Barron* [1979] even correlated the width of the *U* shape to the resulting energetic proton spectrum. *Heckman* [1979] noted that this technique was in use at the Space Environment Services Center (the predecessor of NOAA SWPC), and *Thompson and Secan* [1979] noted that the U.S. Air Force considered that "the requirement for reliable predictions of high-energy solar events was a primary driving force behind the installation of SOON/RSTN" (Solar Optical Observing Network/Radio Solar Telescope Network). But a later analysis by *Cliver et al*. [1985] demonstrated that the microwave radio method was flawed and would miss SEP events, while producing an unacceptably large false alarm rate.

Apparently, the first quasi-operational SEP forecasting technique was the "proton prediction system" (PPS76), an event-oriented empirical technique described by *Smart and Shea* [1979] based on average SEP intensity-time profiles, peak intensities, and event durations. The output was a SEP time-intensity profile, and it was driven by solar flare parameters (either microwave or X-ray) and flare location. Continued updates and improvements to the technique have been reported by *Smart and Shea* [1989] and *Kahler et al*. [2007].

Another long-standing empirical model is *protons*, in use at NOAA SWPC since 1979 [*Heckman et al*., 1992] and updated by *Balch* [1999, 2008]. Similar to PPS, the *protons* model is based on the association of solar flares with SEP events, and input parameters for the prediction model are the time-integrated soft X-ray flux, peak soft X-ray flux, and the location of the associated flare. Additionally, the occurrence or nonoccurrence of metric radio type II and type IV bursts is taken into account. The *protons* model predicts the probability of a ≥10 MeV proton event, the delay time until onset, and the time of the maximum, all with respect to the maximum of the X-ray flare. *Balch* [2008] examined the predictions by the *protons* model for 127 SEP events between 1986 and 2004 (he excluded an additional 28 events where the flare was believed to have occurred behind the solar limb). The technique does not issue warnings or alerts in an automated manner—rather, it is used as an informational tool by a human forecaster. Balch concluded that there was room for improvement in the technique, and he also foresaw the inclusion of CME parameters as proxies for the shock near the Sun at some point in the future to improve the predictions.

Recently, numerous novel techniques have appeared in the literature. *Posner* [2007] utilized a *van Hollebeke et al*. [1975] observation that relativistic electrons are the first in situ sign of a SEP event. Using archival data from SOHO Comprehensive Suprathermal and Energetic Particle Analyser (COSTEP)/Electron Proton Helium

Instrument (EPHIN) [*Müller-Mellin et al*., 1995], Posner demonstrated that a reliable short-term prediction of the resulting SEP proton intensity was available 30–60 min before the onset of 30–50 MeV protons with an average warning time of ~63 min. The technique was rebranded as Relativistic Electron Alert System for Exploration (REleASE) and made available online (e.g., http://iswa.gsfc.nasa.gov) whenever the SOHO COSTEP data are available in near real time [*Posner et al*., 2009].

Núñez [2011] described a dual-module empirical forecasting technique called *UMASEP-10* that was tested against all ≥10 MeV SEP events in solar cycles 22 and 23. The real-time input is soft X-ray, proton fluxes, and flare location information. SEP probabilities are sorted depending on the magnetic connectivity of the source region as being "well connected" or "poorly connected." The technique does not rely on CME-driven shock properties (e.g., type II radio bursts). The archival detection probability was about 80%, with a false alarm rate of 34%, and it was claimed to outperform the human forecasting. The warning time was defined as the time between the issuance of a UMASEP warning and the time that the GOES ≥10 MeV surpassed the 10 pfu threshold; the average warning time reported for all events in the archival study was a little more than 5 h, and it dropped to 65 min for well-connected events. *Núñez* [2015] has extended the technique with an additional forecasting tool for higher-energy (>100 MeV) protons called *UMASEP-100*, which is based on the correlation between derivatives of the soft X-ray flux and the proton flux.

For the highest-energy SEP protons that penetrate Earth's atmosphere and activate ground-based cosmic ray detectors, the ground-level event (GLE) Alert Plus technique was recently reported by *Souvatzoglou et al*. [2014]. GLEs are a subset of about 10% of all SEP events [e.g., *Mewaldt et al*., 2012], but they represent the most energetic ions. Based on an archival study of the most recent 13 GLEs, the GLE Alert Plus technique produced alarms for 12 events (with 1 miss) from 8 to 52 min before the NOAA SWPC alerts (based on crossing the 10 pfu threshold for ≥10 MeV). The authors noted that in two cases limited real-time warnings have been issued using this technique.

We are aware that additional forecasting techniques have been described in the literature, but they do not appear to be actively in use. *Laurenza et al*. [2009] described an improvement to the SWPC *protons* technique based on flare location, flare size, and the time-integrated intensity of low-frequency radio type III bursts at 1 MHz, which they interpreted as evidence of particle acceleration/escape. The 1 MHz frequency of the radio burst corresponds to escaping electrons at a radial distance ~7 R_{Sun} from Sun center. Their technique does not produce an estimate of SEP peak intensity or total fluence; but based on a study of archival data from 1995 to 2005, they claimed a probability of detection of 63%, with a false alarm rate of 42% and an average warning time of ~55 min. This study also excluded events where the associated activity was behind the solar limb.

Kane and Lin [1979] reported that >20 min advance warning of SEPs was possible from space-based monitoring of hard X-rays. *Gabriel and Patrick* [2003] described a neural network-prediction system based on daily and hourly averages of long and short X-ray wavelengths, rather than flares. They claimed a 65% success rate with a high false alarm rate (21%) for a 48 h prediction, but the technique was apparently not put into operational use. *Garcia* [2004a, 2004b] described results of archival SEP forecasting based on the soft (2004a) and hard (2004b) X-ray spectra of flares. The hard X-ray technique was based on earlier reports by *Heckman et al*. [1992] and *Kiplinger* [1995], who noted the association of SEP events with a "soft-hard-harder" spectral behavior. Work by *Grayson et al*. [2009] provided additional evidence for this using Reuven Ramaty High Energy Solar Spectroscopic Imager observations, but *Kahler* [2012] was much less supportive. *Kubo and Akioka* [2004] suggested that a threshold in the duration of the X-ray flare was required for the appearance of SEPs. *Valach et al*. [2011] described a neural network-based SEP prediction scheme based on the usual X-ray and type II/IV radio signatures but also included information about the associated CME. *Huang et al*. [2012] described an ensemble approach to SEP prediction, combining solar flare and CME measurement models.

Other prediction schemes claiming many days' advance warning of "proton flares" (as SEP-associated eruptive events were called initially) have appeared in the literature [e.g., *Krivsky*, 1972; *Severny et al*., 1979]. A novel technique offering a 24 h warning of large flares and SEPs based on solar magnetic field measurements was described by *Falconer et al*. [2011, 2012]. It is based on vector magnetograph measurements of active regions, so it is most reliable when they are within 30° of the Sun's central meridian [*Falconer et al*., 2014]. Forecasters can use the technique to determine if an active region is capable of producing SEPs in the days

leading up to the time it becomes magnetically well connected to Earth (or any other solar system object). Of course, if the active region magnetic fields grow or subside as it nears the western limb then measurements obtained near central meridian will not be relevant. Similarly, attempts to correlate SEP probabilities with magnetic information about active regions obtained near the Sun's central meridian [e.g., *McIntosh*, 1990] suffer from foreshortening effects when the regions are near the solar limbs.

For decades researchers have noted that the key observations of CMEs low in the corona are not available in real time for assessment of SEP production [e.g., *Rust*, 1982; *Heckman et al*., 1992; *Laurenza et al*., 2009; *Kahler and Ling*, 2015; *Nunez*, 2015; *Marsh et al*., 2015]. This is because of limitations of telemetering data from space: the two primary space-based platforms with suitable coronagraphs (SOHO and STEREO) provide only thinly sampled observations with latency delays that make them unsuitable to provide warnings for CME-producing SEPs. As a result, those observations have been too sparse and too late to provide useful SEP warnings to operators of space-based infrastructure, as well as to robotic and human space explorers. With the installation of the new K-Cor coronagraph at Mauna Loa Solar Observatory, those limitations have been significantly reduced for several hours on many days, and the instrument offers a test bed for the possibility of expansion to an operational system.

3. Observations of the 1/2 January 2016 CME and Associated SEP

On 1 January 2016, Active Region #2473 (located at S21 W89) erupted with an M2-level soft X-ray flare at ~23:05 UT (peak ~00:11 UT on 2 January). The region had been magnetically classified as "beta-gamma-delta" 4 days earlier but was downgraded to "beta" in the days before this event. Prior to the M2 event there was a B6 X-ray flare peaking at 20:21 UT and a C3 flare at 22:30 UT, both tagged to that region. A weak type III radio burst starting ~22:28 UT seen by Wind/WAVES [*Bougeret et al*., 1995] also accompanied the C3 flare. The M2 flare was accompanied by type II/IV radio emission starting at 23:21 UT (SWPC report), and a type III was evident in Wind/WAVES and STEREO SWAVES-A [*Bougeret et al*., 2008] starting ~23:16 UT.

The GOES 13 $\geq$10 MeV proton intensity began rising at geosynchronous orbit at ~00 UT on 2 January and peaked at 21 particles/cm^2 s sr (reaching the threshold for a "minor" radiation storm) at 04:50 UT. SEP observations by SOHO's COSTEP/EPHIN instrument revealed that both the C3 flare and type III were associated with the emission of 0.3–1 MeV relativistic electrons that arrived at SOHO as a weak event around 22:40 UT, and the M2 flare/type III resulted in a more conspicuous electron event at ~23:32 UT. The 4.3–51 MeV/n ion onset of this event shows clear energy dispersion in SOHO observations for both protons and helium nuclei, with ~5 MeV/n ions arriving at 1 AU at ~01:30 UT. A preceding, much weaker ion event also appears in SOHO and (at lower ion energies) in ACE/Ultra Low Energy Isotope Spectrometer observations about 1 h earlier. Both ion events seem linked with the relativistic electron events, but only the stronger event reaches the threshold for a $\geq$10 MeV radiation storm.

A fast CME associated with this eruption was detected by the ground-based K-Cor coronagraph at Mauna Loa Solar Observatory, as well as by SOHO LASCO; there were no STEREO observations of the event because of the hiatus in operations during the solar conjunction. Example images of the event at the Sun are shown in Figure 1, and the GOES 15 X-rays, Wind/WAVES radio, and SOHO COSTEP measurements are shown in Figure 2. The GOES SEP event is shown in Figure 3a, with a zoom of a 2 h span showing the coronagraph height-time measurements for the CME superposed in Figure 3b.

The white-light corona has been imaged daily at Mauna Loa Solar Observatory since 1980 [e.g., *Fisher et al*., 1981; *Elmore et al*., 2003; *St. Cyr et al*., 2015a]. In late 2013 the new K-Cor coronagraph was deployed [*de Wijn et al*., 2012] as part of the proposed COronal Solar Magnetism Observatory suite [*Tomczyk et al*., 2016]. K-Cor permits measurements very close to the solar disk (1.05–3.0 R_{Sun}) with high spatial resolution and high temporal cadence. For the CME described here, K-Cor images were acquired about every 15 s from 22:33 UT on 1 January 2016 to 00:40 UT on 2 January. There was a small data gap from 23:26 UT to 23:41 UT, late in the CME transit, but it did not impede efforts to obtain measurements of the speed of the leading edge of the CME low in the corona. The data gap was due to a calibration sequence, initiated because the observer was not aware that a CME was in progress. The CME leading edge was no longer visible when observations resumed.

K-Cor first detected a depletion in the white-light intensity low in the corona above the SW limb starting at ~22:55 UT. The CME leading edge (a loop) was first measurable at ~1.5 R_{Sun} at 23:00 UT, and movement

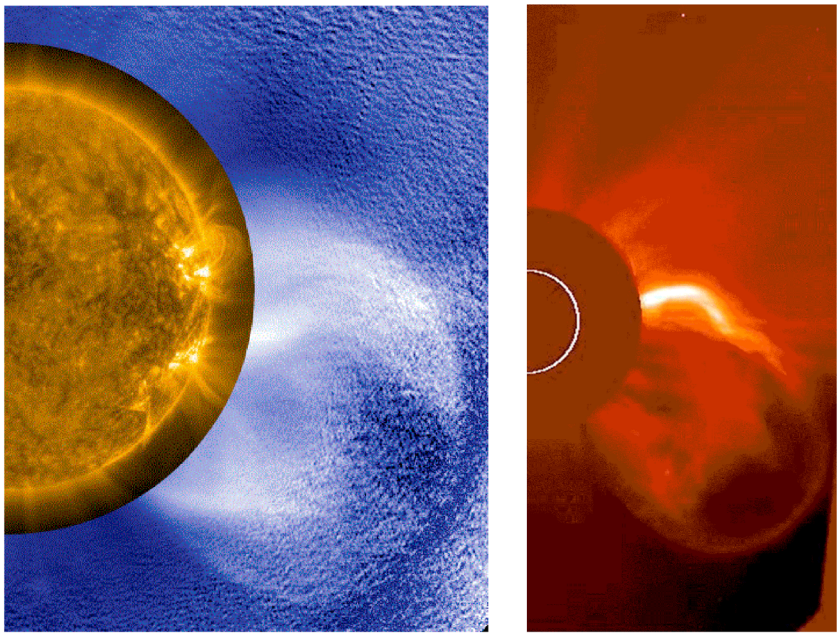

Figure 1. (left) A composite image from SDO AIA (193 Å) on 1 January 2016 at 23:26 UT and MLSO K-Cor at 23:24 UT. The CME leading edge is at a height ~2.5 R_{Sun}. (right) SOHO LASCO C2 image from 2 January 2016 at 00:00 UT showing the CME leading edge at 6.5 R_{Sun}. The size and relative location of the solar disk are indicated by the white circle superposed on the shadow of the coronagraph occulting disk.

was detected within a few minutes. Using 10 min K-Cor observation early in the transit (23:07 UT to 23:17 UT), the leading edge of the loop rose from 1.6 to 2.2 R_{Sun}, yielding a speed of ~520 km/s. Measurements continued in K-Cor until the data gap, at which point SOHO LASCO C2 first detected the leading edge of the loop at a height of 2.7 R_{Sun} at 23:24 UT. An initial acceleration of ~1500 m/s^2 was measured in the first few minutes, the combined K-Cor and LASCO C2 height-time measurements indicated acceleration (~370 m/s^2), and the final speed of the event in C2 was ~1700 km/s at 6.5 R_{Sun}. The CME could be tracked to 29 R_{Sun} in the LASCO C3 field of view.

The event was brighter than the coronal and stray-light background, so it was visible in direct (as opposed to differenced) images of both K-Cor and LASCO C2. The central position angle of the CME in K-Cor was 245°, and the event subtended a width of 74°. The K-Cor and C2 height measurements align well (within 0.15 R_{Sun}), assuming a small (8°) clockwise rotation of the field between the two instruments. The primary CME was somewhat wider (90°) in LASCO C2, and a faint shock developed by ~02:00 UT in LASCO C3 creating a full 360° halo event [e.g., *St. Cyr et al.*, 2005].

On a typical observing day, much of the K-Cor data is transmitted over the open Internet from Mauna Loa Solar Observatory (MLSO) to the High Altitude Observatory in Boulder, where it is processed and available online with a 5–15 min latency. Thus, if the K-Cor data stream had been monitored at MLSO on 1 January 2016, for the appearance of a fast CME, then by ~23:15 UT a warning could have been issued that there was a high probability of an impending SEP event since the active region near the SW limb was likely magnetically well connected to Earth.

4. Comparison of SEP Warnings for the 1/2 January 2016 Event

In Table 1 we compare the SEP warning time for the 1 January 2016 event afforded by several techniques, in the order the warnings have been or would have been issued. With the exception of UMASEP and the NOAA records, the techniques have been performed retrospectively on archival data and would have a delay from latency of the data that is not included in the table. The two earliest warnings would have been issued from CME observation methods, with the MLSO K-Cor being first. Based on a series of consecutive images of the CME, we believe that a reliable estimate of the speed would have been available from K-Cor by 23:17 UT.

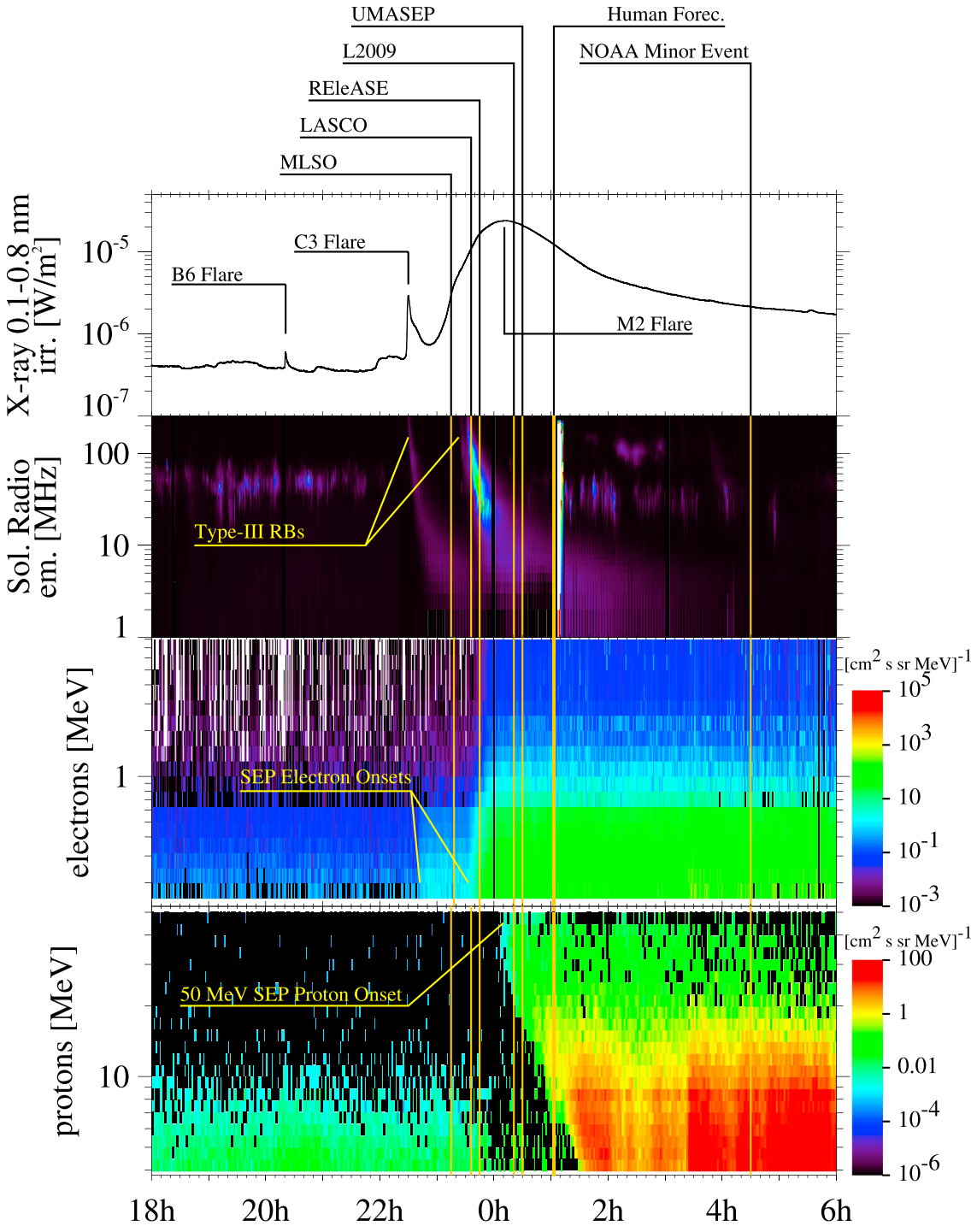

Figure 2. (top to bottom) Time series of GOES soft X-rays, solar radio emissions (Wind/WAVES), 0.3–8 MeV relativistic electrons, and the 4–50 MeV protons (SOHO COSTEP). The data are described in the "Observations" section, and the demarcations of SEP forecasts are described in the "Comparison of CME alerts" and Table 1.

For this event, K-Cor provided a warning 19 min before the SOHO/LASCO C2 coronagraph, which observed the CME later in its transit through the middle corona.

The leading edge of the CME was first detected by SOHO LASCO C2 at a height of 2.7 R_{Sun} at 23:24 UT, just peeking above the occulting disk; thus, it was optimal for early detection of this event by LASCO. During this period, the C2 coronagraph was obtaining images every 12 min. The fastest time that LASCO C2 can expose, read out, and compress (lossy) a full-resolution, full-field image would decrease the time between images

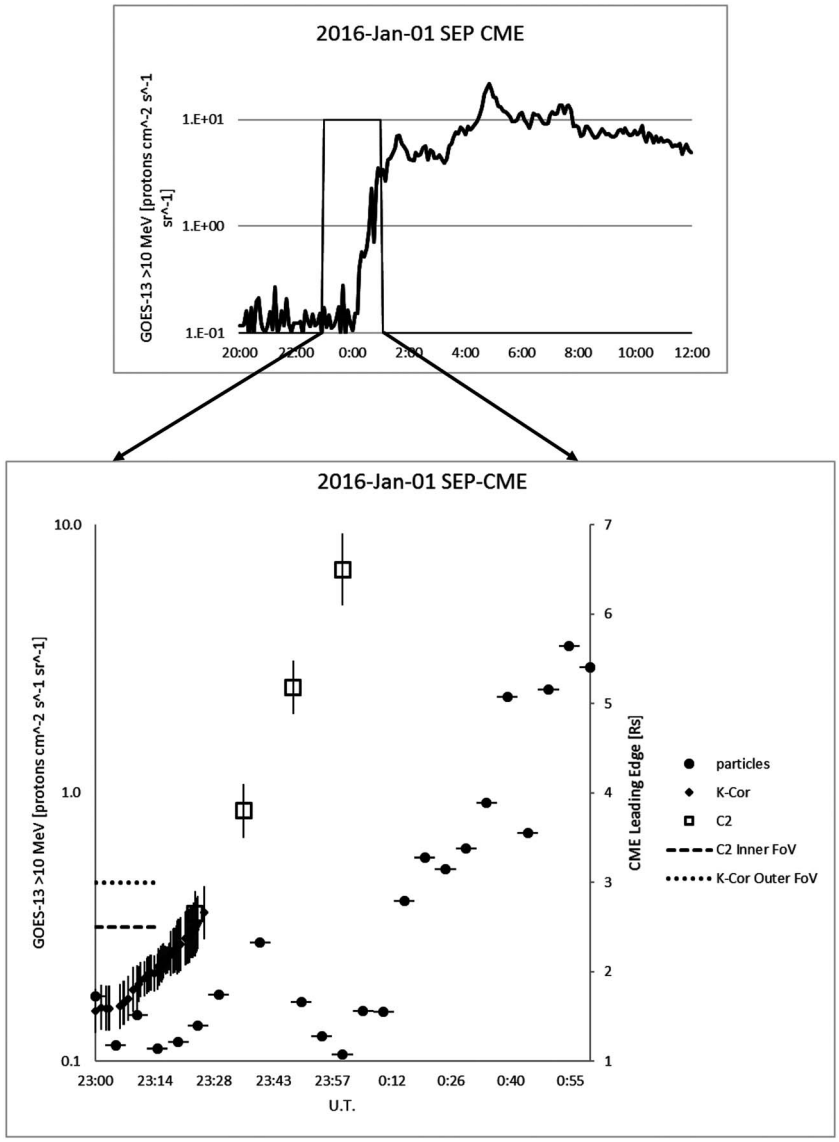

Figure 3. Two plots showing increasing time resolution of the 1 January 2016 event. (top) The GOES ≥10 MeV proton time series. (bottom) The height-time measurements at full resolution (~15 s) from K-Cor, at 12 min resolution from LASCO C2, and at 5 min for the GOES ≥10 MeV protons.

from 12 min to ~5 min (K. Schenk, personal communication, 2016). The SOHO spacecraft and ground segment were designed to spend large portions of each day (~19 out of every 24 h) in real-time contact during the nominal 2.5 year mission in order to support the interactive commanding and the high data continuity requirement of helioseismology [*St. Cyr et al.*, 1995]. But the spacecraft recently celebrated its 20th anniversary on orbit, and data recorder downlinks from SOHO now occur every 6–8 h, at best. While that is acceptable latency to provide warning time for appearance of Earth-directed CMEs and to forecast the onset of geomagnetic storms, the infrequent downlinks make that platform unsuitable for SEP warning from LASCO and COSTEP. The 1 January 2016 event occurred during such a DSN gap.

After the coronagraph warnings, there are three techniques that are based on particles escaping near the Sun. The REleASE forecast, while active several times each day when SOHO is in contact with NASA's Deep Space Network (DSN), also had to be reconstructed from archival data as the event occurred during a DSN gap. This technique creates a 60 min forecast of the upcoming proton intensity every minute from the latest in situ observations of relativistic electrons in the solar wind near Earth. A warning would have been issued at 23:45 UT when the forecast (28.2–50.1 MeV) proton intensity exceeds a threshold value, in

Table 1. Comparison of SEP Warning Times for 1 January 2016 Event[a]

Technique	Comments	Assuming *R/T* Data Stream
MLSO K-Cor	Fast CME (520 km/s)	1 January at 23:17 UT[e]
SOHO LASCO C2	Fast CME (1700 km/s)	1 January at 23:36 UT[e]
RELeASE[b]	Relativistic electrons	1 January at 23:45 UT[e]
Laurenza[c]	Flare location, X-ray, and radio	2 January at 00:21 UT[e]
UMASEP[d]	X-ray and proton flux	2 January at 00:44 UT
NOAA 10 MeV warning	Human forecaster	2 January at 01:03 UT
NOAA "minor" SEP event	≥10 MeV protons exceed 10 particles/cm^2 s sr	2 January at 04:30 UT

[a]The bottom two rows in Table 1 represent the actual times that these activities occurred. The UMASEP prediction was available in near real time. The RELeASE and Laurenza entries were determined from archival data, as were the coronagraph estimates.
[b]J. Labrenz, personal communication [*Posner*, 2007].
[c]M. Laurenza, personal communication [*Laurenza et al*., 2009].
[d]M. Núñez, personal communication [*Núñez*, 2011].
[e]Latency of observations not included.

this case 0.1/(cm^2 s sr MeV), which is approximately 2.2 pfu from the 28.2–50.1 MeV proton energy interval. The forecast maximum proton intensity for the January 2016 event is ~0.2/(cm^2 s sr MeV) for ~40 MeV protons, and the actual measurement shows that ~0.1/(cm^2 s sr MeV) was reached during the event.

It is important to point out that SEP event protons (according to our definition, excluding ESPs) have two phases during the onset: an exponential increase, here (Figure 3 lasting from 00:00 UT to ~01:00 UT, which is followed by a more gradual rise (~01:00 UT–05:00 UT). While the exponential increase can be rapid, the gradual phase can be very irregular and slow. Therefore, particle forecasting techniques that depend on particle intensity such as UMASEP may issue late forecasts if the maximum forecast intensity is close to the forecasting threshold. On the other hand, such events, even if well connected to Earth, often allow ample forecasting time between flare/CME onset and crossing a proton intensity threshold—5 h in this case before crossing the 10 pfu threshold in this case. A counterexample is the 20 January 2006 event, where thresholds were crossed within ~20 min, still during the exponential rise.

REleASE uses electron intensity and a rise parameter (a measure of how fast the electron intensity rises). In this case the electron technique provided a prompt forecast, despite the maximum proton intensity being very close to the threshold, which is driven by the rise parameter. Similar to the coronagraph technique, REleASE is also independent from observations of processes hidden behind the solar limb. Note that in this case the maximum intensity of the flare occurs *after* the REleASE forecast is issued.

The forecast by the *Laurenza et al*. [2009] technique that is based on the presence of type III radio burst, and the location and intensity of the X-ray flare, would have been issued approximately 10 min after the maximum of the flare. In this case, as there was a type III radio burst, and a well-connected flare of magnitude exceeding M2, this would be at or around 00:21 UT. The delay of this technique over the others is driven by the slowly rising flare time profile.

As discussed earlier, UMASEP [*Núñez*, 2011] depends on flare X-rays and the presence of a proton enhancement for a warning. While the flare signal in this case came from the Earth-facing side of the Sun, the late 00:44 UT forecast is likely due to low statistics in the number of protons arriving at GOES early in the event. Núñez (personal communication, 2016) has commented, "It is important to say that for this event in particular, the correlation analysis between the X-ray and the proton fluxes yielded a low correlation estimation (but enough to issue a forecast). This low correlation, contributed to predict a low-intensity SEP event forecast (i.e., 56 pfu at most)." UMASEP would certainly provide earlier forecast for stronger, i.e., more relevant SEP events, in which the proton detection threshold falls in an earlier phase of the exponential rise.

The *Falconer et al*. [2014] technique was in hiatus on 1 January 2016, but measurements on archival data when Active Region 2473 was near central meridian (several days before the event described here) showed that the proxy for free magnetic energy was 30 kG, which was above average and indicated some potential for flaring and a fast CME (Falconer, personal communication, 2016). From Figure 5 of the *Falconer et al*. [2014] paper it appears that this value for the proxy corresponds to ~3% (~10%) chance of a fast CME based on no prior flaring (prior flaring) of the active region.

The SWPC SEP *protons* prediction model, conducted by a human forecaster in the loop, uses as input the above-mentioned flare observations and examines the presence or absence of type II and type IV radio emission. The NOAA SWPC Solar and Geophysical Activity Summary for that day reports type II emission accompanying the M2 flare from 23:10 UT to 00:11 UT, and this was likely based on metric radio emission. The SWPC warning was issued at 01:03 UT; the actual crossing of the 10 pfu threshold occurs at 04:30 UT, during the late, more gradual rise phase of the event.

The coronagraph-based alert for the SEP onset for this event offered a clear temporal advantage over all other techniques. Other than pre-event-based techniques [e.g., *Posner et al*., 2014] it may be the only forecast that can be made before the actual onset of the SEP injection at the Sun. All other techniques in Table 1 are triggered after particle release occurs at the Sun. A limitation to the coronagraph technique may be the false alarm rate for even fast CMEs that are not associated with SEPs. As described above, this can be at least partially mitigated by the presence of DH radio emissions. The actual false alarm rate using the coronagraph technique can be estimated in a statistical analysis of many events, as shown in *Gopalswamy et al*. [2008], Figures 10 and 11. Of course, one could empirically couple one or more of the above techniques with the CME technique to improve the forecasting capability beyond the warning of an event to SEP intensity, duration, spectral characteristics, etc. In the next section we discuss other observations that may mitigate this apparent limitation of the technique.

5. Discussion

The single case for the 1 January 2016 event described above demonstrates that a reasonable SEP warning from the K-Cor coronagraph was possible for this event, but is it statistically representative? Given the *Gopalswamy et al*. [2008] report discussed earlier, it is easy to imagine a coronagraph-driven "stoplight" warning system, tuned to a user's sensitivity to the onset of SEP events. Currently, there are no near-Earth space assets with the capability to provide near-real-time reports of the appearance of DH radio bursts, but the STEREO beacon of S/WAVES is still active at the time of this writing.

Similar to almost all studies of the relationship between SEPs and CMEs, the speeds in *Gopalswamy et al*. [2008] were measured in SOHO LASCO's field of view of the middle-outer corona, so there were no measurements of the initial CME accelerations, which are likely relevant for this discussion. The speed of the 1 January 2016 CME as measured in K-Cor was in the top 15% of events reported for the inner corona [*St. Cyr et al*., 1999, 2015a], but significant acceleration was only evident early in the K-Cor field of view. That acceleration was about half the largest value measured in archival data for the inner corona [*St. Cyr et al*., 1999]. Using measurements from the entire LASCO field of view (to 29 R_{Sun}), the CME displayed a much smaller acceleration (~60 m/s^2) than in the low corona. This is not surprising because about half of the CMEs show deceleration in the middle-outer corona [e.g., *Yashiro et al*., 2004]. Significant positive acceleration in CMEs has been difficult to measure when using only middle-outer corona observations [e.g., *St. Cyr et al*., 2000]. *MacQueen and Fisher* [1983] found that accelerations could be measured in the small sample of 12 CMEs, where observations from MLSO Mk3 of the inner corona and SMM C/P [*MacQueen et al*., 1980] observations of the middle corona were combined. *St. Cyr et al*. [1999] expanded and demonstrated that acceleration could be measured in a majority of CMEs when combining observations from those same two instruments for more than 140 CMEs observed from 1980 to 1989. Estimates of the initial acceleration of CMEs associated with GLE events using a flare-onset technique indicated that large values of acceleration may be possible, and the MLSO observation of the CME associated with the 2 November 2003 GLE event had an acceleration of 2400 m/s^2 [*Gopalswamy et al*., 2012].

Other researchers have found similar results. *Vrsnak* [2001] reported that most of the 48 CMEs in his study attained maximum acceleration below ~4 R_{Sun}. Using a sample of 95 STEREO CMEs observed during 2007–2010, *Bein et al*. [2011] reported that 74% of the impulsive events in their study reached peak acceleration below 1.5 R_{Sun}; a similar result was reported by *Temmer et al*. [2010]. *Joshi and Srivastava* [2011] studied the acceleration of six well-observed STEREO CMEs in 3-D, and they concluded that the maximum acceleration of the leading edge of those events occurred inside of 2 R_{Sun}. *Kocharov et al*. [2001a, 2001b] claimed that even the residual acceleration detected in LASCO was sufficient to categorize SEP events, but *Kahler* [2003] contested that claim since most of the

acceleration occurred in the low corona, beneath the LASCO occulting disk. The perils of extrapolating CME locations, timing, and association with other activity based on measurements made in the middle-outer corona have been well documented [e.g., *MacQueen*, 1985; *Mancuso*, 2007].

What about extreme events? We can examine the archive of extremely fast CMEs to estimate the advance warning a coronagraph could provide if higher-cadence images were available. Apparently, the fastest CME detected by any of the MLSO coronagraphs in the inner corona was an east limb event on 7 September 2005, with a speed of 2490 km/s and an associated SEP event [*Ling et al*., 2014]. In the online LASCO CME catalogue [*Yashiro et al*., 2004] there are a dozen CMEs with speed >2500 km/s in the middle-outer corona, and the highest speed measured in over 20 years' observation is ~3500 km/s (see also *Riley* [2012] for a discussion of extreme CME speeds). An extremely fast event like that would move almost 0.3 R_{Sun} per minute, so high image cadence (e.g., ~1 min) low in the corona appears to be beneficial if not necessary for an SEP onset warning.

What about the range of possible warning times from a coronagraph? It is well accepted that SEPs from eruptive events in the western hemisphere of the Sun arrive more quickly at Earth than those in the east because they are better magnetically connected [e.g., *van Hollebeke et al*., 1975]. We can look at recent studies based on archival data to estimate the range of warning times possible. *Kahler* [2013] examined a large sample of SOHO LASCO CMEs associated with 20 MeV SEPs, and he defined "TO" as the time from the extrapolated CME launch at 1 R_{Sun} to the time of the SEP onset at the 1 AU platform *Wind*. He found that events from magnetically well-connected longitudes (W62°–W90°) had a median TO of 1.7 h. Using L1 platforms and the twin STEREO spacecraft, *Richardson et al*. [2014] reported delays of ~54 min between well-connected solar events (as measured by the onset of type III radio emissions) and the appearance of 14–24 MeV protons. *Kahler and Ling* [2015] reported that the average delay time from the peak of the X-ray flare to the 10 pfu onset of the SEP event for the best-connected events (W57–W75) was 1.55 h with a sigma of 2.9 h. Despite the differences in the instrumentation, techniques, and temporal resolutions among these studies, we believe that the results are in reasonable agreement and indicative of the range of warning times possible from a coronagraph-based technique. It is important to note that when comparing advance warning times across techniques, they rather strongly depend on the energy threshold of the ions being forecast because of the increasing propagation time of ions from the Sun with decreasing energy.

Another approach is to ask when the particles are released compared to the CME location in the low corona. Since the CME position is available at the speed of light, and at least the lower-energy SEPs are subrelativistic, then there is some gain available. Of course, if protons with higher kinetic energy (velocity) are produced, the warning time decreases. *Posner* [2007] calculated that the difference in arrival times between relativistic electrons and 30 MeV protons is about 30 min, whereas it is only 5 min for 300 MeV protons. These are, of course, minimum delays and dependent on magnetic connection and propagation conditions. Several researchers have calculated estimates of the time of solar particle release in the corona based on their velocity dispersion [e.g., *Kahler*, 1994; *Tylka et al*., 2003; *Reames*, 2009; *Gopalswamy et al*., 2012], and *Klassen et al*. [2002] reported that the mildly relativistic electrons in their study were released when the associated type II burst and CME were within 5 R_{Sun}. Despite the variety of techniques, most conclude that the particles are initially released when the CME is traversing heights from ~2 to 4 R_{Sun}.

Plasma diagnostics of CME shocks low in the corona [*Giordano et al*., 2013] were measured routinely by the SOHO UltraViolet Coronagraph Spectrometer instrument [*Kohl et al*., 1995]. For example, *Ciaravella et al*. [2005] reported measurements of a fast CME in the low corona that was accompanied by an SEP event. Their analysis indicated that the particles were released below 4 R_{Sun}; MLSO Mk4 data for that event (not included in their report) showed that the leading edge of the CME was, in fact, below 2 R_{Sun}. Additionally, *Gopalswamy et al*. [2013] identified shock locations in the low corona in a survey of 32 CMEs with type II radio bursts. They reported a range of 1.20–1.93 R_{Sun} (average 1.43 R_{Sun}) when comparing the locations of CMEs and the starting time of the radio bursts. This work was expanded to 59 CMEs with SEPs and type II radio bursts by *Makela et al*. [2015]. These findings reiterate that measurements of the dynamics of a CME as low as possible in the corona would add valuable time to an SEP warning.

We noted in the event description that the loop CME on 1 January 2016 was first measurable at 1.5 R_{Sun}, despite the K-Cor field of view starting much lower in the corona, just above the photosphere. In fact, this

case is rather typical, whereby a CME first becomes visible at an altitude above ~1.3 R_{Sun}. More than 60% of the initial measurement height of Mk3 CMEs from 1980 to 1989 reported by *St. Cyr et al.* [1999] were between 1.3 and 1.7 R_{Sun} with an average first measurement at a height of 1.51 R_{Sun}. Since some CMEs were detected near the inner boundary of the Mk3 field of view we can conclude that the limitation was not an instrumental effect. The most likely explanation is that many CMEs are only first visible at this height, similar to the report by *Gibson et al*. [2006] describing observations of the magnetic structures of quiescent prominence cavities prior to eruption. A similar situation is found in recent EUV surveys of cavities prior to eruption [e.g., *Forland et al*., 2013; *Karna et al*., 2015]. *Gopalswamy et al*. [2012] assumed an initial height of 1.25 R_{Sun} for the CME at liftoff. This question of the height of CME formation, while intriguing, is beyond the scope of this manuscript, but we note it as being relevant to the discussion of coronagraphic warnings of impending SEP events.

As early as *van Hollebeke et al*. [1975], it was clear that a significant fraction of all SEPs came from the farside of the Sun since they could not be associated with a flare or eruption. The coronagraph and the relativistic electron techniques offer an advantage to many prediction techniques when an eruption is on the Sun's farside. The Thomson scattering function (by which we see the white light corona) is symmetric with respect to the plane of the sky [e.g., *Hundhausen*, 1993]. The ability of an individual coronagraph to detect activity away from the sky-plane (i.e., on the visible disk and behind the limb) is frequently quantified as the "visibility function" of the instrument [*Webb and Howard*, 1994]. *Tripathi et al*. [2004] reported that 92% of EUV posteruptive arcades in a 5 year period had associated SOHO LASCO CMEs, including those on the visible disk, far from the plane of the sky. This indicates that the number of CMEs from the Sun's farside that were undetected by LASCO was extremely small. An example of this capability is the detection of extremely fast CMEs visible from eruptions on the farside of the Sun in the days prior to the beginning of the Halloween 2003 violent activity [*National Oceanic and Atmospheric Administration, National Weather Service*, 2004]. Ongoing work to confirm the high LASCO visibility function for CMEs using STEREO observations at quadrature to the Sun-Earth line have been reported by *St. Cyr et al*. [2015b].

One apparent limitation of the coronagraph-based SEP warning is that it only provides warning of the onset, at least as of this writing. But there are reports that may provide new avenues to research. *Kahler and Vourlidas* [2005] examined a sample of 31 west limb CMEs with similar speeds and found that those classified as "SEP rich" were brighter (i.e., higher electron densities) than those that were "SEP poor," and they were more likely to be associated with streamer blowouts. Confirming a report by *Gopalswamy et al*. [2004], they also noted that preceding coronal activity was commonplace prior to a SEP-rich CME. For the 1 January 2016 event described in this paper, several CMEs were visible in LASCO in the hours before the event, and the SEP-associated CME did appear to disrupt a small existing streamer. Further, based on the classification in *St. Cyr et al*. [2015a], the CME was considered a "bright" event since it was visible in direct images.

Recent reports by *Gopalswamy et al*. [2015, 2016] indicate a relationship between CME initial acceleration and the power law index of the subsequent SEP fluence spectrum. They reported that eruptive events with low acceleration produce the softest spectra, while those with the highest CME acceleration are associated with GLEs that have hard spectra. Many of the CME accelerations were based on LASCO C2 measurements in the middle corona, so it is possible that additional information about the nature of the SEP events may be available from CME measurements even lower in the corona. We have recently searched the archive of 36 years' MLSO observation of the inner corona, and we have identified many (>80) fast CMEs with associated SEP events. We will report on the comparison of their initial acceleration and expansion with SEP characteristics in the near future.

6. An Idealized Coronagraph SEP Warning System

MLSO K-Cor is a scientific research instrument, but we can imagine modest modifications to be able to use it in a quasi-operational fashion several hours per day. One would need to capture the digital data stream at the observatory and implement software-based CME detection, measurement, and warning schemes. Examples of these software applications exist; in fact, the automated detection and measurement of CMEs in archival data have become commonplace in recent years, and various technical approaches appear to have reasonable levels of success [e.g., *Webb and Howard*, 2012; *Robbrecht and Berghmans*, 2005]. Numerous software routines in the refereed literature include CACTUS [*Robbrecht et al*., 2009], SEEDS [*Olmedo et al*., 2008],

ARTEMIS [*Boursier et al*., 2009], CORIMP [*Byrne et al*., 2012], and AICMED [*Tappin et al*., 2012]. Reports describing additional CME detection techniques include *Qu et al*. [2006], *Nieniewski* [2008], *Young and Gallagher* [2008], and *Rigozo* [2012]. Following detection and initial measurement of a fast CME, an electronic warning could be sent to the end-user, who could then examine the K-Cor data and other solar activity indicators and forecasting techniques, to verify that the warning was not a false alarm.

Where would one deploy a truly operational coronagraph SEP warning system? There are obvious advantages and disadvantages to ground-based versus space-based platforms, and there are several locations to consider for the latter. The benefits of a ground-based system are likely lower cost compared to space, as well as the ability to maintain and upgrade the telescopes. The necessity of multiple sites to provide full-time coverage is a liability, but *Leibacher and the GONG Project Team* [1999] reported that the Global Oscillations Network Group had achieved a 90% observational duty cycle for helioseismology studies with six longitudinally separated ground-based sites. The experience of several decades' observation at MLSO demonstrates that the inner corona can be routinely monitored using a ground-based high-altitude telescope, but it is unlikely that the middle-outer corona can be routinely observed given the high level of scattered light in the sky.

Turning to space-based platforms, one can examine the track record of solar remote sensing instruments that have flown in low-Earth orbit (LEO), LEO-Sun-synchronous, geosynchronous (GEO), and heliocentric orbits. Instruments in equatorial or slightly inclined LEO undergo day-night transitions 15 times per day. The Sun is eclipsed for 30–40 min during each ~90 min orbit, making the duty cycle for detecting fast CMEs rather poor. The P78-1 (SOLWIND; described in *Sheeley et al*. [1980]) and Coriolis (Solar Mass Ejection Imager; described in *Eyles et al*. [2003]) spacecraft both flew in LEO-Sun-synchronous orbit, but no coronagraphs have flown in GEO orbit. Both of those orbits offer long (e.g., months) durations of solar observations, punctuated by eclipse seasons of several weeks as the orbital plane precesses through the course of a year. The Solar Dynamics Observatory in GEO has exceeded its 95% data capture requirement during at least 22 of the 72 day observing windows [*Pesnell et al*., 2012]. The success of SOHO, ACE, and Wind at the Lagrangian L1 point demonstrate stable locations that are relatively near Earth, without eclipses. This is also true for the 1 AU heliocentric drift orbits of STEREO, which also maintain high duty cycles, but coronagraphs in these orbits suffer from telemetry constraints due to the challenges of deep space communications.

There is an important caveat to the cadence determination for space-based coronagraphs. The cosmic ray background adds an unwanted noise level to imaging devices in space [e.g., *Pike and Harrison*, 2000], which is usually tolerated by sound optical and engineering design in the total signal-to-noise budget. But when SEP storms strike, high-energy ionizing protons can completely mask the faint coronal signals in the CCDs [e.g., *Posner et al*., 2014]. For the LASCO coronagraphs on SOHO the impact of the energetic proton storms on the CCD detectors can overwhelm the coronal signal and cause a "whiteout" for hours to, in extreme cases, days. There are other negative effects beyond the poor image quality. The additional random intensity spikes in the image due to the SEP storm cause the onboard compression algorithm, which has been optimized for nominal image quality, to require more processing time and result in less compression. These two negative impacts can in turn overflow the telemetry as well as wreak havoc with the onboard schedule of image acquisition. The STEREO heliospheric imagers, however, have utilized onboard software routines to remove most of this sporadic background before the image is compressed and put into the telemetry stream for downlink. Further, it appears that the STEREO coronagraphs may be less susceptible to proton storms than SOHO LASCO because the exposure times are a factor of ~10 shorter, and the data transfer times from the CCDs are also significantly shorter.

Although the physics of optical systems does not preclude a single instrument covering a wide range of coronal heights (say from 1.1 R_{Sun} to more than 10 R_{Sun}), the present-day technology of detectors does not have sufficient dynamic range to accommodate the extreme radial gradient in brightness that exists in the Thomson-scattered corona. Therefore, we do not believe that a single coronagraph can simultaneously satisfy requirements for both rapid measurements low in the solar atmosphere (for SEP warnings) and less frequent measurements of CMEs far from the Sun (for geomagnetic storm forecasting). This is evident from the design philosophy adopted for the SOHO LASCO suite of coronagraphs as well as for the STEREO Sun Earth Connection Coronal and Heliospheric Investigation suite. In both cases nested fields of view with overlap were necessary in order to optimize spatial resolution of coronal features, the time scales of dynamic events at different altitudes above the Sun's photosphere, and to accommodate the large radial gradient in coronal brightness.

7. Conclusion

We have reported here a conceptual coronagraph-based SEP warning technique. The near-real-time availability of the 1 January 2016 observations demonstrates that the primary component of a prototype ground-based system for SEP onset warnings is available several hours on most days. A comparison of the coronagraph-based SEP warning time for this event with other existing techniques shows that a significant temporal advantage for forecasting an SEP onset can be achieved.

We also initiated the discussion of an implementation for a more robust coronagraph-based SEP warning system. Given the limitations of present-day technology, the requirements for a coronagraph to measure the early dynamics of CMEs in the inner corona in order to provide timely SEP warnings will restrict the outer field of view of the instrument. To track the motion of CMEs in the middle-outer corona in order to forecast the arrival time of energetic storm particles and geomagnetic storms will likely require different optical instrumentation.

As documented in *St. Cyr et al*. [2014], the impact of having routine SOHO LASCO coronagraphic observations of our star's atmosphere has been broad across the breadth of pure and applied heliophysic science topics. Reiterating the sentiment stated in closing that paper, we have presented another argument for "the international science community and the forecasting community (to) work together to secure these measurements in the future to support this broad range of research across the field of heliophysics."

Acknowledgments

The initial idea to investigate a coronagraph-based SEP warning technique came from a discussion with N. Zapp and D. Fry, both of NASA-JSC. Several individuals have contributed through discussions or assistance in data analysis: T. Alberti, C. Balch, D. Falconer, B. Heber, L. Jian, S. Kahler, J. Labrenz, M. Laurenza, G. Michalek, M. Nunez, I. Richardson, S. St. Cyr, K. Schenk, B.J. Thompson, R. Wimmer-Schweingruber, H. Xie, and S. Yashiro. MLSO data are freely available online courtesy of the Mauna Loa Solar Observatory (www2.hao.ucar.edu/mlso), operated by the High Altitude Observatory, as part of the National Center for Atmospheric Research (NCAR). NCAR is supported by the National Science Foundation. *SOHO* is a project of international cooperation between ESA and NASA. *SOHO* LASCO data are freely available online, and CME data were taken from the CDAW LASCO catalog. This CME catalog is generated and maintained at the CDAW Data Center by NASA and the Catholic University of America in cooperation with the Naval Research Laboratory. SDO data are courtesy of the NASA/SDO and the AIA, EVE, and HMI science teams. The authors thank the reviewers for their constructive comments. The authors are not aware of any conflicts of interest relating to the content of this manuscript.

References

Anderson, K. A., R. Arnoldy, R. Hoffman, L. Peterson, and J. R. Winckler (1959), Observations of low-energy solar cosmic rays from the flare of 22 August 1958, *J. Geophys. Res.*, *64*, 1133–1147, doi:10.1029/JZ064i009p01133.

Arnoldy, R. L., R. A. Hoffman, and J. R. Winckler (1960), Solar cosmic rays and soft radiation observed at 5,000,000 kilometers from Earth, *J. Geophys. Res.*, *65*, 3004–3007, doi:10.1029/JZ065i009p03004.

Bailey, D. K. (1957), Disturbances in the lower ionosphere observed at VHF following the solar flare of 23 February 1956 with particular reference to auroral-zone absorption, *J. Geophys. Res.*, *62*, 431–463, doi:10.1029/JZ062i003p00431.

Bakshi, P., and W. Barron (1979), Prediction of solar flare proton spectral slope from radio burst data, *J. Geophys. Res.*, *84*, 131–137, doi:10.1029/JA084iA01p00131.

Balch, C. C. (1999), SEC proton prediction model: verification and analysis, *Radiat. Meas.*, *30*, 231–250.

Balch, C. C. (2008), Updated verification of the Space Weather Prediction Center's solar energetic particle prediction model, *Space Weather*, *6*, S01001–13, doi:10.1029/2007SW000337.

Bein, B. M., S. Berkebile-Stoiser, A. M. Veronig, M. Temmer, N. Muhr, I. Kienreich, D. Utz, and B. Vrsnak (2011), Impulsive acceleration of coronal mass ejections. I. Statistics and coronal mass ejection source region characteristics, *Space Sci. Rev.*, *738*, 191–205, doi:10.1088/0004-637X/738/2/191.

Bougeret, J. L., et al. (1995), WAVES: The radio and plasma wave investigation on the Wind spacecraft, *Space Sci. Rev.*, *71*, 231–263.

Bougeret, J. L., et al. (2008), S/WAVES: The radio and plasma wave investigation on the STEREO mission, *Space Sci. Rev.*, *136*, 487–528, doi:10.1007/978-0-387-09649-0_16.

Boursier, Y., P. Lamy, A. Llebaria, F. Goudail, and S. Robelus (2009), The ARTEMIS catalog of LASCO coronal mass ejections, *Sol. Phys.*, *257*, 125–147, doi:10.1007/s11207-009-9370-5.

Brueckner, G. E., et al. (1995), The Large Angle Spectroscopic Coronagraph (LASCO), *Sol. Phys.*, *162*, 357.

Byrne, J. P., H. Morgan, S. R. Habbal, and P. T. Gallagher (2012), Automatic detection and tracking of coronal mass ejections: II. Multiscale filtering of coronagraph images, *Astrophys. J.*, *752*, 145–157, doi:10.1088/0004-637X/752/2/145.

Cane, H. V., D. V. Reames, and T. T. von Rosenvinge (1988), The role of interplanetary shocks in the longitudinal distribution of solar energetic particles, *J. Geophys. Res.*, *93*, 9555–9567, doi:10.1029/JA093iA09p09555.

Cane, H. V., W. C. Erickson, and N. P. Prestage (2002), Solar flares, type III radio bursts, coronal mass ejections, and energetic particles, *J. Geophys. Res.*, *107*(A10), 1315, doi:10.1029/2001JA000320.

Castelli, J. P., J. Aarons, and G. A. Michael (1967), Flux density measurements of radio bursts of proton producing and nonproton flares, *J. Geophys. Res.*, *72*, 5491–5498, doi:10.1029/JZ072i021p05491.

Castelli, J. P., and W. R. Barron (1977), A catalogue of solar radio bursts 1966–1976 having spectral characteristics predictive of proton activity, *J. Geophys. Res.*, *82*, 1275–1278, doi:10.1029/JA082i007p01275.

Ciaravella, A., J. C. Raymond, S. W. Kahler, A. Vourlidas, and J. Li (2005), Detection and diagnostics of a coronal shock wave driven by a partial-halo coronal mass ejection on 2000 June 28, *Astrophys. J.*, *621*, 1121–1128.

Cliver, E. W., L. F. McNamara, and L. C. Gentile (1985), Peak flux density spectra of large solar radio bursts and proton emission from flares, *J. Geophys. Res.*, *90*, 6251–6266, doi:10.1029/JA090iA07p06251.

Cliver, E. W., S. W. Kahler, and D. V. Reames (2004), Coronal shocks and solar energetic proton events, *Astrophys. J.*, *605*, 902–910.

Cliver, E. W., A. G. Ling, A. Belov, and S. Yashiro (2012), Size distributions of solar flares and solar energetic particle events, *Astophys. J. Lett.*, *756*, L29–L32, doi:10.1088/2041-8205/756/2/L29.

Cohen, C. M. S., R. A. Mewaldt, A. C. Cummings, R. A. Leske, and E. C. Stone (2001), Forecasting the arrival of shock-accelerated solar energetic particles at Earth, *J. Geophys. Res.*, *106*, 20,979–20,983, doi:10.1029/2000JA000216.

Dalla, S., et al. (2003), Properties of high heliolatitude solar energetic particle events and constraints on models of acceleration and propagation, *Geophys. Res. Lett.*, *30*(19), 8035, doi:10.1029/2003GL017139.

de Wijn, A. G., J. T. Burkepile, S. Tomczyk, P. Nelson, P. Huang, and D. Gallagher (2012), Stray light and polarimetry considerations for the COSMO K-coronagraph, *Proc. SPIE*, *8444*.

Dierckxsens, M., K. Tziotziou, S. Dalla, I. Patsou, M. S. Marsh, N. B. Crosby, O. Malandraki, and G. Tsiropoula (2015), Relationship between solar energetic particles and properties of flares and CMEs: Statistical analysis of solar cycle 23 events, *Sol. Phys.*, *290*, 841–874, doi:10.1007/s11207-014-0641-4.

Dresing, N., R. Gomez-Herrero, A. Klassen, B. Heber, Y. Kartavykh, and W. Droge (2012), The large longitudinal spread of solar energetic particles during the 17 January 2010 solar event, *Sol. Phys.*, *281*, 281–300.

Elmore, D. F., J. T. Burkepile, J. A. Darnell, A. R. Lecinski, and A. L. Stanger (2003), Calibration of a ground-based solar coronal photometer, in Polarimetry in Astronomy, S. Fineschi, editor, *Proc. of SPIE*, *4843*, 66–75.

English, R. A., R. E. Benson, J. V. Bailey, and C. M. Barnes (1973), Apollo experience report—Protection against radiation, NASA Technical Note D-7080.

Eyles, C. J., G. M. Simnett, M. P. Cooke, B. V. Jackson, A. Buffington, P. P. Hick, N. R. Waltham, J. M. King, P. A. Anderson, and P. E. Holladay (2003), The solar mass ejection imager (SMEI), *Sol. Phys.*, *217*, 319–347.

Falconer, D., A. F. Barghouty, I. Khazanov, and R. Moore (2011), A tool for empirical forecasting of major flares, coronal mass ejections, and solar particle events from a proxy of active-region free magnetic energy, *Space Weather*, *9* S04003, doi:10.1029/2009SW000537.

Falconer, D. A., R. L. Moore, A. F. Barghouty, and I. Khazanov (2012), Prior flaring as a complement to free magnetic energy for forecasting solar eruptions, *Astrophys. J.*, *757*, 32–37, doi:10.1088/0004-637X/757/1/32.

Falconer, D. A., R. L. Moore, A. F. Barghouty, and I. Khazanov (2014), MAG4 versus alternative techniques for forecasting active region flare productivity, *Space Weather*, *12*, 306–317, doi:10.1002/2013SW001024.

Fisher, R. R., R. H. Lee, R. M. MacQueen, and A. I. Poland (1981), New Mauna Loa coronagraph systems, *Appl. Optics*, *20*, 1094.

Forbush, S. E. (1946), Three unusual cosmic-ray increases possibly due to charged particles from the Sun, *Phys. Rev.*, *70*, 771–772.

Forland, B. C., S. E. Gibson, J. B. Dove, L. A. Rachmeler, and Y. Fan (2013), Coronal cavity survey: Morphological clues to eruptive magnetic topologies, *Sol. Phys.*, *288*, 603–615, doi:10.1007/s11207-013-0361-1.

Gabriel, S. B., and G. J. Patrick (2003), Solar energetic particle events: Phenomenology and prediction, *Space Sci. Rev.*, *107*, 55–62.

Garcia, H. A. (2004a), Forecasting methods for occurrence and magnitude of proton storms with solar soft X rays, *Space Weather*, *2* S02002, doi:10.1029/2003SW000001.

Garcia, H. A. (2004b), Forecasting methods for occurrence and magnitude of proton storms with solar hard X rays, *Space Weather*, *2* S06003-13, doi:10.1029/2003SW000035.

Gibson, S. E., D. Foster, J. Burkepile, G. de Toma, and A. Stanger (2006), The calm before the storm: The link between quiescent cavities and coronal mass ejections, *Astron. J.*, *641*, 590–605.

Giordano, S., A. Ciaravella, J. C. Raymond, Y.-K. Ko, and R. Suleiman (2013), UVCS/SOHO catalog of coronal mass ejections from 1996 to 2005: Spectroscopic properties, *J. Geophys. Res. Space Physics*, *118*, 967–981, doi:10.1002/jgra.50166.

Gopalswamy, N., S. Yashiro, S. Krucker, G. Stenborg, and R. A. Howard (2004), Intensity variation of large solar energetic particle events associated with coronal mass ejections, *J. Geophys. Res.*, *109*, A12105, doi:10.1029/2004JA010602.

Gopalswamy, N., S. Yashiro, S. Akiyama, P. Makela, H. Xie, M. L. Kaiser, R. A. Howard, and J. L. Bougeret (2008), Coronal mass ejections, type II radio bursts, and solar energetic particles in the SOHO era, *Ann. Geophys.*, *26*, 3033–3047.

Gopalswamy, N., H. Xie, S. Yashiro, S. Akiyama, P. Makela, and I. G. Usoskin (2012), Properties of ground level enhancement events and the associated solar eruptions during solar cycle 23, *Space Sci. Rev.*, *171*, 23–60, doi:10.1007/s11214-012-9890-4.

Gopalswamy, N., et al. (2013), Height of shock formation in the solar corona inferred from observations of type II radio bursts and coronal mass ejections, *Adv. Space Res.*, *51*, 1981–1989.

Gopalswamy, N., P. Makela, S. Akiyama, S. Yashiro, H. Xie, N. Thakur, and S. W. Kahler (2015), Large solar energetic particle events associated with filament eruptions outside active regions, *Astrophys. J.*, *806*, 8–24, doi:10.1088/0004-637X/806/1/8.

Gopalswamy, N., S. Yashiro, N. Thakur, P. Makela, H. Xie, and S. Akiyama (2016), The 2012 July 23 backside event: An extreme energetic particle event?, *Astron. J.*, in press.

Gosling, J. T., E. Hildner, R. M. MacQueen, R. H. Munro, A. I. Poland, and C. L. Ross (1974), Mass ejections from the Sun: A view from Skylab, *J. Geophys. Res.*, *79*, 4581–4587, doi:10.1029/JA079i031p04581.

Grayson, J. A., S. Krucker, and R. P. Lin (2009), A statistical study of spectral hardening in solar flares and related solar energetic particle events, *Astron. J.*, *707*, 1588–1594, doi:10.1088/0004-637X/707/2/1588.

Heckman, G. R. (1979), Predictions of the Space Environment Services Center, in *Solar-Terrestial Predictions Proceedings*, vol. 1, edited by R. F. Donnelly, pp. 322–349, U.S. Dep. of Commer., Boulder, Colo.

Heckman, G. R., J. M. Kunches, and J. H. Allen (1992), Prediction and evaluation of solar particle events based on precursor information, *Adv. Space Res.*, *12*(2–3), 313–320.

Huang, X., H.-N. Wang, and L.-P. Li (2012), Ensemble prediction model of solar proton events associated with solar flares and coronal mass ejections, *Res. Astron. Astrophys.*, *12*, 313–321.

Hundhausen, A. J. (1993), Sizes and locations of coronal mass ejections: SMM observations from 1980 and 1984–1989, *J. Geophys. Res.*, *98*, 13,177–13,200, doi:10.1029/93JA00157.

Jackman, C. H., E. L. Fleming, and F. M. Vitt (2000), Influence of extremely large solar proton events in a changing stratosphere, *J. Geophys. Res.*, *105*, 11,659–11,670, doi:10.1029/2000JD900010.

Joshi, A. D., and N. Srivastava (2011), Acceleration of coronal mass ejections from three-dimensional reconstruction of STEREO images, *Astron. J.*, *739*, 8–20, doi:10.1088/0004-637X/739/1/8.

Kahler, S. W. (1994), Injection profiles of solar energetic particles as functions of coronal mass ejection heights, *Astron. J.*, *428*, 837–842.

Kahler, S. W. (2001), The correlation between solar energetic particle peak intensities and speeds of coronal mass ejections: Effects of ambient particle intensities and energy spectra, *J. Geophys. Res.*, *106*, 20,947–20,955, doi:10.1029/2000JA002231.

Kahler, S. W. (2003), Energetic particle acceleration by coronal mass ejections, *Adv. Space Res.*, *32*, 2587–2596.

Kahler, S. W. (2012), Solar energetic particle events and the Kiplinger effect, *Astron. J.*, *747*, 66–76, doi:10.1088/0004-637X/747/1/66.

Kahler, S. W. (2013), A comparison of solar energetic particle event timescales with properties of associated coronal mass ejections, *Astron. J.*, *769*, 110–120, doi:10.1088/0004-637X/769/2/110.

Kahler, S. W., E. Hildner, and M. A. I. van Hollebeke (1978), Prompt solar proton events and coronal mass ejections, *Sol. Phys.*, *57*, 429–443.

Kahler, S. W., N. R. Sheeley Jr., R. A. Howard, M. J. Koomen, D. J. Michels, R. E. McGuire, T. T. von Rosenvinge, and D. V. Reames (1984), Associations between coronal mass ejections and solar energetic particle events, *J. Geophys. Res.*, *89*, 9683–9693, doi:10.1029/JA089iA11p09683.

Kahler, S. W., and A. Vourlidas (2005), Fast coronal mass ejection environments and the production of solar energetic particle events, *J. Geophys. Res.*, *110*, A12S01, doi:10.1029/2005JA011073.

Kahler, S. W., E. W. Cliver, and A. G. Ling (2007), Validating the proton prediction system (PPS), *J. Atmos. Sol. Terr. Phys.*, *69*, 43–49, doi:10.1016/j.jastp.2006.06.009.
Kahler, S. W., and A. Ling (2015), Dynamic SEP event probability forecasts, *Space Weather*, *13*, 665–675, doi:10.1002/2015SW001222.
Kallenrode, M.-B. (1993), Neutral lines and azimuthal "transport" of solar energetic particles, *J. Geophys. Res.*, *98*, 5573–5591, doi:10.1029/92JA02778.
Kane, S. R., and R. P. Lin (1979), Prediction of solar proton events using hard X-ray emission, in *Solar -Terrestrial Predictions Proceedings*, vol. III, edited by R. F. Donnelly, pp. D-34–35, U.S. Dep. of Commer., Boulder, Colo.
Karna, N., W. D. Pesnell, and J. Zhang (2015), Appearances and statistics of coronal cavities during the ascending phase of solar cycle 24, *Astron. J.*, *810*, 123–128, doi:10.1088/0004-637X/810/2/123.
Kim, M.-H., et al. (2014), Comparison of Martian surface ionizing radiation measurements from MSL-RAD with Badhwar-O'Neill 2011/HZETRN model calculations, *J. Geophys. Res. Planets*, *119*, 1311–1321, doi:10.1002/2013JE004549.
Kiplinger, A. L. (1995), Comparative studies of hard X-ray spectral evolution in solar flares with high-energy proton events observed at Earth, *Ap. J.*, *453*, 973–986.
Klassen, A., V. Bothmer, G. Mann, M. J. Reiner, S. Krucker, A. Vourlidas, and H. Kunow (2002), Solar energetic electron events and coronal shocks, *A & A*, *385*, 1078–1088, doi:10.1051/0004-6361:20020205.
Kocharov, L., J. Torsti, O. C. S. Cyr, and T. Huhtanen (2001a), A relation between dynamics of coronal mass ejections and production of solar energetic particles, *A&A*, *370*, 1064–1070.
Kocharov, L., J. Torsti, and O. C. S. Cyr (2001b), The role of CME dynamics in production of ~10 MeV protons, *ProcICRC*, *2001*, 3435–3438.
Kohl, J. L., et al. (1995), The ultraviolet coronagraph spectrometer for the Solar and Heliospheric Observatory, *Sol. Phys.*, *162*, 313–356.
Krivsky, L. (1972), Prediction of proton flares and Forbush effects, in *Solar Activity Observations and Predictions, Progress in Astronautics and Aeronautics*, vol. 30, edited by P. S. McIntosh and M. Dryer, pp. 389–409, M.I.T. Press, Cambridge, Mass.
Kubo, Y., and M. Akioka (2004), Existence of thresholds in proton flares and application to solar energetic particle alerts, *Space Weather*, *2* S01002-6, doi:10.1029/2003SW000022.
Lario, D., N. E. Raouafi, R.-Y. Kwon, J. Zhang, R. Gomez-Herrero, N. Dresing, and P. Riley (2014), The solar energetic particle event on 2013 April 11: An investigation of its solar origin and longitudinal spread, *Ap. J.*, *797*, 8–23, doi:10.1088/0004-637X/797/1/8.
Lario, D., et al. (2016), Longitudinal properties of a widespread solar energetic particle event on 2014 February 25: Evolution of the associated CME shock, *Ap. J.*, *819*, 72–94, doi:10.3847/0004-637X/819/1/72.
Laurenza, M., E. W. Cliver, J. Hewitt, M. Storini, A. G. Ling, C. C. Balch, and M. L. Kaiser (2009), A technique for short-term warning of solar energetic particle events based on flare location, flare size, and evidence of particle escape, *Space Weather*, *7*, S04008, doi:10.1029/2007SW000379.
Leibacher, J. W., and the GONG Project Team (1999), The Global Oscillation Network Group (GONG) Project, *Adv. Space Res.*, *24*, 173–176.
Ling, A. G., D. F. Webb, J. T. Burkepile, and E. W. Cliver (2014), Development of a current sheet in the wake of a fast coronal mass ejection, *Astron. J.*, *784*, 91–104, doi:10.1088/0004-637X/784/2/91.
MacQueen, R. M. (1985), Coronal mass ejections: Acceleration and surface associations, *Sol. Phys.*, *95*, 359–361.
MacQueen, R. M., and R. R. Fisher (1983), The kinematics of solar inner coronal transients, *Sol. Phys.*, *89*, 89–102.
MacQueen, R. M., A. Csoeke-Poekh, E. Hildner, L. House, R. Ryenolds, A. Stanger, H. Tepoel, and W. Wagner (1980), The High Altitude Observatory coronagraph/polarimeter on the Solar Maximum Mission, *Sol. Phys.*, *65*, 91–107.
Makela, P., N. Gopalswamy, S. Akiyama, H. Xie, and S. Yashiro (2015), Estimating the height of CMEs associated with a major SEP event at the onset of the metric type II radio burst during solar cycles 23 and 24, *Astrophys. J.*, *806*, 13–24, doi:10.1088/0004-637X/806/1/13.
Mancuso, S. (2007), Coronal transients and metric type II radio bursts, *A&A*, *463*, 1137–1141.
Marsh, M. S., S. Dalla, M. Dierckxsens, T. Laitinen, and N. B. Crosby (2015), SPARX: A modeling system for solar energetic particle radiation space weather forecasting, *Space Weather*, *13*, 386–394, doi:10.1002/2014SW001120.
McCracken, K. G. (1962), The cosmic ray flare effect, *J. Geophys. Res.*, *67*, 447–458, doi:10.1029/JZ067i002p00447.
McGuire, R. E., M. A. I. van Hollebeke, and N. Lal (1983), A multi-spacecraft study of the coronal and interplanetary transport of solar cosmic rays, I Introduction and observations, in Proc. 18th Int. Cosmic Ray Conf., vol. 10, pp. 353–356, Bangalore, India.
McIntosh, P. (1990), The classification of sunspot groups, *Sol. Phys.*, *125*, 251–267.
McKenna-Lawlor, S., P. Goncalves, A. Keating, G. Reitz, and D. Matthia (2012), Overview of energetic particle hazards during prospective manned missions to Mars, *Planet. Space Sci.*, *63–64*, 123–132.
Mertens, C. J., B. T. Kress, M. Wiltberger, S. R. Blattnig, T. S. Slaba, S. C. Solomon, and M. Engel (2010), Geomagnetic influence on aircraft radiation exposure during a solar energetic particle event in October 2003, *Space Weather*, *8*, S03006, doi:10.1029/2009SW000487.
Mewaldt, R. A., M. D. Looper, C. M. S. Cohen, D. K. Haggerty, A. W. Labrador, R. A. Leske, G. M. Mason, J. E. Mazur, and T. T. von Rosenvinge (2012), Energy spectra, composition, and other properties of ground-level events during solar cycle 23, *Space Sci. Rev.*, *171*, 97–120.
Müller-Mellin, R., et al. (1995), COSTEP—Comprehensive Suprathermal and Energetic Particle Analyser, *Sol. Phys.*, *162*, 483–504.
National Oceanic and Atmospheric Administration, National Weather Service (2004), Service assessment: Intense space weather storms October 19–November 07, 2003, NOAA, National Weather Service, Silver Spring, Md.
National Research Council (2008), Managing space radiation risk in the new era of space exploration.
Nieniewski, M. (2008), Detection and tracking of coronal mass ejections (CMEs) by means of the watershed segmentation and Hough transform, Proc. World Congress on Engineering, vol 1, London.
Núñez, M. (2011), Predicting solar energetic proton events ($E > 10$ MeV), *Space Weather*, *9*, 1–28, doi:10.1029/2010SW000640.
Núñez, M. (2015), Real-time prediction of the occurrence and intensity of the first hours of >100 MeV solar energetic proton events, *Space Weather*, *13*, 807–819, doi:10.1002/2015SW001256.
Olmedo, O., J. Zhang, H. Wechsler, A. Poland, and K. Borne (2008), Automatic detection and tracking of coronal mass ejections in coronagraph time series, *Sol. Phys.*, *248*, 485–499, doi:10.1007/s11207-007-9104-5.
Pesnell, W. D., B. J. Thompson, and P. C. Chamberlin (2012), The Solar Dynamics Observatory, *Sol. Phys.*, *275*, 3–15, doi:10.1007/s11207-011-9841-3.
Pickering, J. E., and J. M. Talbot (1963), A reappraisal of the radiation hazards to manned space flight, in Proceedings of the 2nd Manned Space Flight Meeting, Dallas, TX, Am. Inst. of Aeronautics and Astronautics, New York, 22–24 Apr.
Pike, C. D., and R. A. Harrison (2000), Long-duration cosmic ray modulation from a Sun-Earth L1 orbit, *Astron. Astrophys.*, *362*, L21–L24.
Posner, A. (2007), Up to 1 hour forecasting of radiation hazards from solar energetic ion events, *Space Weather*, *5*, 1–28, doi:10.1029/2006SW000268.
Posner, A., V. Bothmer, H. Kunow, B. Heber, R. Muller-Mellin, J.-P. Delaboudiniere, B. J. Thompson, G. E. Bruckner, R. A. Howard, and D. J. Michels (1997), Fluxes of MeV particles at Earth's orbit and their relationship with the global structure of the solar corona:

Observations from SOHO, in the Proc. 31st ESLAB Symp., "Correlated Phenomena at the Sun, in the Heliosphere, and in Geospace," ESA SP-415.
Posner, A., S. Guetersloh, B. Heber, and O. Rother (2009), A new trend in forecasting solar radiation hazards, *Space Weather*, *7*, 1–2, doi:10.1029/2009SW000476.
Posner, A., M. Hesse, and O. C. S. Cyr (2014), The main pillar: Assessment of space weather observational asset performance supporting nowcasting, forecasting, and research to operations, *Space Weather*, *12*, 257–276, doi:10.1002/2013SW001007.
Prew, H. E. (1956), Space exploration—The new challenge to the electronics industry, in Proceedings of the American Astronautical Society, 3rd annual meeting, New York, 6–7 Dec.
Prise, A. J., L. K. Harra, S. A. Matthews, D. M. Long, and A. D. Aylward (2014), An investigation of the CME of 3 November 2011 and its associated widespread solar energetic particle event, *Sol. Phys.*, *289*, 1731–1744, doi:10.1007/s11207-013-0435-0.
Qu, M., F. Y. Shih, J. Jing, and H. Wang (2006), Automatic detection and classification of coronal mass ejections, *Sol. Phys.*, *237*, 419–431, doi:10.1007/s11207-006-0114-5.
Reames, D. V. (2000), Particle acceleration by CME-driven shock waves, in Proc. 26th Intl. Cosmic Ray Conf., edited by B. L. Dingus, pp. 289–300, Am. Inst. Phys.
Reames, D. V. (2009), Solar release times of energetic particles in ground-level events, *Astron. J.*, *693*, 812–821, doi:10.1088/0004-637X/693/1/812.
Reid, G. C. (1972), Ionospheric effects of solar activity, in *Solar Activity Observations and Predictions, Progress in Astronautics and Aeronautics*, vol. 30, edited by P. S. McIntosh and M. Dryer, pp. 293–312, M.I.T. Press, Cambridge, Mass.
Richardson, I. G., T. T. von Rosenvinge, H. V. Cane, E. R. Christian, C. M. S. Cohen, A. W. Labrador, R. A. Leske, R. A. Mewaldt, M. E. Wiedenbeck, and E. C. Stone (2014), >25 MeV proton events observed by the high energy telescopes on the STEREO A and B spacecraft and/or at the Earth during the first ~seven years of the STEREO mission, *Sol. Phys.*, *289*, 3059–3107, doi:10.1007/s11207-014-0524-8.
Rigozo, N. R. (2012), Automatic detection method of coronal mass ejection by digital image analysis, *Rev. Bras. Geogr.*, *30*, 103–110.
Riley, P. (2012), On the probability of occurrence of extreme space weather events, *Space Weather*, *10*, S02012-23, doi:10.1029/2011SW000734.
Robbrecht, E., and D. Berghmans (2005), Entering the era of automated CME recognition: A review of existing tools, *Sol. Phys.*, *228*, 239–251.
Robbrecht, E., D. Berghmans, and R. A. M. Van der Linden (2009), Automated LASCO CME catalog for solar cycle 23: Are CMEs scale invariant?, *Astron. J.*, *691*, 1222–1234, doi:10.1088/0004-637X/691/2/1222.
Rouillard, A. P., et al. (2011), Interpreting the properties of solar energetic particle events by using combined imaging and modeling of interplanetary shocks, *Ap. J.*, *735*, 7–17, doi:10.1088/0004-637X/735/1/7.
Rouillard, A. P., et al. (2012), The longitudinal properties of a solar energetic particle event investigated using modern solar imaging, *Ap. J.*, *752*, 44–64, doi:10.1088/0004-637X/752/1/44.
Rust, D. M. (1982), Solar flares, proton showers, and the space shuttle, *Science*, *216*(4549), 939–946.
Severny, A. B., N. N. Stepanyan, and N. V. Steshenko (1979), Soviet short-term forecasts of active region evolution and flare activity, in *Solar-Terrestial Predictions Proceedings*, vol. 1, edited by R. F. Donnelly, pp. 72–88, U.S. Department of Commerce, Boulder, Colo.
Sheeley, N. R., Jr., D. J. Michels, R. A. Howard, and M. J. Koomen (1980), Initial observations with the SOLWIND coronagraph, *Astrophys. J.*, *237*, L99–L101.
Souvatzoglou, G., A. Papaioannou, H. Mavromichalaki, J. Dimitroulakos, and C. Sarlanis (2014), Optimizing the real-time ground level enhancement alert system based on neutron monitor measurements: Introducing GLE Alert Plus, *Space Weather*, *12*, 623–649, doi:10.1002/2014SW001102.
Smart, D. F., and M. A. Shea (1979), PPS76—A computerized "event mode" solar proton forecasting technique, in *Solar-Terrestial Predictions Proceedings*, vol. 1, edited by R. F. Donnelly, pp. 406–427, U.S. Dep. of Commer., Boulder, Colo.
Smart, D. F., and M. A. Shea (1989), PPS-87: A new event oriented solar proton prediction model, *Adv. Space Res.*, *9*(10), 281–284.
St. Cyr, O. C., L. Sanchez-Duarte, P. C. H. Martens, J. B. Gurman, and E. Larduinat (1995), SOHO ground segment, science operations, and data products, *Sol. Phys.*, *162*, 39–59.
St. Cyr, O. C., J. T. Burkepile, A. J. Hundhausen, and A. R. Lecinski (1999), A comparison of ground-based and spacecraft observations of coronal mass ejections from 1980–1989, *J. Geophys. Res.*, *104*, 12,493, doi:10.1029/1999JA900045.
St. Cyr, O. C., et al. (2000), Properties of coronal mass ejections: SOHO LASCO observations from January 1996 to June 1998, *J. Geophys. Res.*, *105*, 18,169, doi:10.1029/93JA03586.
St. Cyr, O. C., R. A. Howard, S. P. Plunkett, G. Lawrence, G. Stenborg, S. Yashiro, G. Michalek, N. Sheeley, N. Gopalswamy, and A. Vourlidas (2005), The last word: The definition of halo coronal mass ejections, *Eos*, *86*(30), 281–282.
St. Cyr, O. C., B. Fleck, and J. M. Davila (2014), The impact of coronagraphs, *Eos*, *95*(41), 369–370.
St. Cyr, O. C., Q. A. Flint, H. Xie, D. F. Webb, J. T. Burkepile, A. R. Lecinski, C. Quirk, and A. L. Stanger (2015a), MLSO *Mark-III* k-coronameter observations of the CME rate from 1989–1996, *Sol. Phys.*, *290*, 2951–2962, doi:10.1007/s11207-015-0780-2.
St. Cyr, O. C., H. Xie, D. Duncan, D. F. Webb, R. Howard, and J. B. Gurman (2015b), Estimating coronagraph visibility functions—Progress report, Transactions of the Amer. Geophys. Union, abstract #SH31C-2425.
Svestka, Z., and P. Simon (1969), Proton Flare Project, 1966, Summary of the August/September particle events in the McMath Region 8461, *Sol. Phys.*, *10*, 3–59.
Tappin, S. J., T. A. Howard, M. M. Hampson, R. N. Thompson, and C. E. Burns (2012), On the autonomous detection of coronal mass ejections in heliospheric imager data, *J. Geophys. Res.*, *117*, A05103, doi:10.1029/2011JA017439.
Temmer, M., A. M. Veronig, E. P. Kontar, S. Krucker, and B. Vrsnak (2010), Combined STEREO/RHESSI study of coronal mass ejection acceleration and particle acceleration in solar flares, *Astron. J.*, *712*, 1410–1420, doi:10.1088/0004-637X/712/2/1410.
Thompson, B. J., S. P. Plunkett, J. B. Gurman, J. S. Newmark, O. C. S. Cyr, and D. J. Michels (1998), SOHO/EIT observations of an Earth-directed coronal mass ejection on May 12, 1997, *Geophys. Res. Lett.*, *25*, 2465–2468, doi:10.1029/98GL50429.
Thompson, R. L., and J. A. Secan (1979), Geophysical forecasting at AFGWC, in *Solar-Terrestial Predictions Proceedings*, vol. 1, edited by R. F. Donnelly, pp. 350–366, U.S. Department of Commerce.
Tomczyk, S., et al. (2016), Scientific objectives and capabilities of the coronal solar magnetism observatory, *J. Geophys. Res. Space Phys.*, *121*, 7470–7487, doi:10.1002/2016JA022871.
Tousey, R., and M. Koomen (1972), Movement of a bright source in the white-light corona, *Bull. AAS*, *4R*, 394.
Tripathi, D., V. Bothmer, and H. Cremades (2004), The basic characteristics of EUV post-eruptive arcades and their role as tracers of corona mass ejection source regions, *Astron. Astrophys.*, *422*, 337, doi:10.1051/0004-6361:20035815.
Tylka, A. J., C. M. S. Cohen, W. F. Dietrich, S. Krucker, R. E. McGuire, R. A. Mewaldt, C. K. Ng, D. V. Reames, and G. H. Share (2003), Onsets and release times in solar particle events, Proceedings of the 28th International Cosmic Ray Conference, 3305–3308.

U.S. Department of Commerce, National Oceanic and Atmospheric Administration, National Weather Service (2004), Service assessment: Intense space weather storms October 19–November 07, 2003.
Valach, F., M. Revallo, P. Hejda, and J. Bochnicek (2011), Predictions of SEP events by means of a linear filter and layer-recurrent neural network, *Acta Astronaut.*, *69*, 758–766.
Van Hollebeke, M. A. I., L. S. Ma Sung, and F. B. McDonald (1975), The variation of solar proton energy spectra and size distribution with heliolongitude, *Sol. Phys.*, *41*, 189–223.
Vrsnak, B. (2001), Dynamics of solar coronal eruptions, *J. Geophys. Res.*, *106*, 25,249–25,259, doi:10.1029/2000JA004007.
Warwick, C. S., and M. W. Haurwitz (1962), A study of solar activity associated with polar-cap absorption, *J. Geophys. Res.*, *67*, 1317–1332, doi:10.1029/JZ067i004p01317.
Webb, D. F., and R. A. Howard (1994), The solar cycle variation of coronal mass ejections and the solar wind mass flux, *J. Geophys. Res.*, *99*, 4201, doi:10.1029/93JA02742.
Webb, D. F., and T. A. Howard (2012), Coronal mass ejections: Observations, *Living Rev. Sol. Phys.*, *9*, 5–83.
Yashiro, S., N. Gopalswamy, G. Michalek, O. C. St. Cyr, S. P. Plunkett, N. B. Rich, and R. A. Howard (2004), A catalog of white light coronal mass ejections observed by the SOHO spacecraft, *J. Geophys. Res.*, *109*, A07105, doi:10.1029/2003JA010282.
Young, C. A., and P. T. Gallagher (2008), Multiscale edge detection in the corona, *Sol. Phys.*, *248*, 457–469, doi:10.1007/s11207-008-9177-9.